NREL
NATIONAL RENEWABLE ENERGY LABORATORY

Load-Direction-Derived Support Structures for Wind Turbines: A Lattice Tower Concept and Preparations for Future Certifications

Preprint

Achim Struve and Torsten Faber
University of Applied Sciences Flensburg

Rick Damiani and Jason Jonkman
National Renewable Energy Laboratory

Thomas Ummenhofer
Karlsruhe Institute of Technology

Presented at the German Wind Energy Conference
Bremen, Germany
October 17–18, 2017

NREL is a national laboratory of the U.S. Department of Energy
Office of Energy Efficiency & Renewable Energy
Operated by the Alliance for Sustainable Energy, LLC

This report is available at no cost from the National Renewable Energy Laboratory (NREL) at www.nrel.gov/publications.

Conference Paper
NREL/CP-5000-69110
November 2017

Contract No. DE-AC36-08GO28308

This report is available at no cost from the National Renewable Energy Laboratory (NREL) at www.nrel.gov/publications.

Available electronically at SciTech Connect http:/www.osti.gov/scitech

Available for a processing fee to U.S. Department of Energy and its contractors, in paper, from:

U.S. Department of Energy
Office of Scientific and Technical Information
P.O. Box 62
Oak Ridge, TN 37831-0062
OSTI http://www.osti.gov
Phone: 865.576.8401
Fax: 865.576.5728
Email: reports@osti.gov

Available for sale to the public, in paper, from:

U.S. Department of Commerce
National Technical Information Service
5301 Shawnee Road
Alexandria, VA 22312
NTIS http://www.ntis.gov
Phone: 800.553.6847 or 703.605.6000
Fax: 703.605.6900
Email: orders@ntis.gov

Cover Photos by Dennis Schroeder: (left to right) NREL 26173, NREL 18302, NREL 19758, NREL 29642, NREL 19795.

NREL prints on paper that contains recycled content.

LOAD-DIRECTION-DERIVED SUPPORT STRUCTURES FOR WIND TURBINES: A LATTICE TOWER CONCEPT AND PREPARATIONS FOR FUTURE CERTIFICATIONS

Achim Struve*, Rick Damiani**, Jason Jonkman**, Torsten Faber*, Thomas Ummenhofer***
* University of Applied Sciences Flensburg, Flensburg, Germany, 0461/48161-111, Achim.Struve@hs-flensburg.de, Faber@hs-flensburg.de
** National Renewable Energy Laboratory, Golden, U.S., Rick.Damiani@nrel.gov, Jason.Jonkman@nrel.gov
*** Karlsruhe Institute of Technology, Karlsruhe, Germany, Thomas.Ummenhofer@kit.edu

Summary

The call for more cost-effective and environmentally friendly tower concepts is motivated by tower costs [1] and tower CO_2-emission contributions [2], which are high relative to the whole wind turbine system. The proposed rotatable tower concept with yaw bearing at the bottom instead of the top of the tower will provide beneficial economic and environmental impacts to the turbine system. This wind alignment capability indicates a load-direction-derived tower design. By combining this approach with a lattice concept, large material and cost savings for the tower can be achieved. This paper presents a way to analyze and verify the proposed design through aero-servo-elastic simulations, which make future certifications of rotatable tower concepts viable. For this reason, the state-of-the-art, open-source lattice-tower finite-element-method (FEM) module SubDyn [10], developed by the National Renewable Energy Laboratory, has been modified to account for arbitrary member cross-sections. Required changes in the beam element stiffness and mass matrix formulation took place according to an energy method [13]. All validated adaptions will be usable within the aero-servo-elastic simulation framework FAST and are also beneficial for other nonrotatable lattice structures.

1. Introduction

1.1 Motivation

The cost of a typical multimegawatt wind turbine support structure, including transport and erection, can amount to more than 30% of the whole turbine system cost [1]. The quest to make wind energy prices more competitive with conventional energy generation calls for more cost-effective solutions. But this is not the only reason why innovative concepts are necessary. Assuming emissions of 2.8 tons of CO_2 per generated ton of steel [2], the production of conventional support structures—which weigh hundreds of tons—causes a large environmental impact. The proposed rotatable tower concept meets both the cost and the environmental challenges.

1.2 The Rotatable Tower Concept

Conventional tower concepts are equipped with a yaw bearing at the top of the tower designed to align the rotor nacelle assembly (RNA) with the wind direction. For this reason, the tower has to withstand equal thrust loads from any direction. In contrast, a rotatable tower concept features a yaw bearing at the ground level of the support structure, which implies that the entire tower is aligned with the wind direction. Furthermore, a fixed tower-to-RNA connection causes different shear forces and bending moments with respect to the local tower coordinate system. By leveraging this difference, tower cross-sections other than circular are conceivable. Significant material and cost savings can be expected because the material can be located only where it is needed. The generated cost savings for the tower have to overcome the increased costs for a yaw bearing at the bottom of the tower, even though environmental benefits can still be expected.

2. Review of Former Approaches

Apart from some historical grain-grinding windmills with a rotatable tower and nacelle assembly [3], a first attempt at decreasing the tower “dam” effect by rotating aerodynamic tower segments in the region of blade passage was suggested by Kleinhenz [4]. This aspect is likewise mentioned in a patent [5]. A recent publication [6] assumes an elliptical tower cross section and presents rough cost estimates for the tower and yaw bearing. Because of its rudimentary approach of a simply scaled conventional yaw bearing, economic benefits could not be observed, but technical feasibility has already been attested. A German company proposes a more detailed yaw bearing concept, which is embedded in the foundation and provides a certain distance between two radial slide bearings [7]. Fundamental statics show hyperbolic radial load reductions, which increase with growing bearing distances. The patent solution of Himmelmann et al. [8] takes advantage of the same principle, but assumes the location of the yaw bearing within the tower. Another problem is the local buckling strength of tubular tower concepts with elongated profiles, where flank-sided shells have low curvature. Therefore, an aerodynamic tower concept is modified to a shell-lattice hybrid approach mentioned in [7]. It consists of two C-profiles at a prescribed distance from each other. Both profiles are connected and stiffened by strut members. Such a concept presents high fore-aft bending stiffness while also using less material, and buckling vulnerable shells at the tower flanks are removed. Lift forces are the result of pressure integration over the surface of the structure. In the case of a hybrid tower, replacing tower-flank sided shells with strut members will cause decreased lift forces. This becomes even more important for high-wind-speed parked/idling design load cases (DLCs) and yaw-drive complications.

3. The Rotatable Lattice Tower

3.1 Structural Characteristics

Regarding the aspects mentioned in the previos section, a rotatable lattice tower is favored by removing the C-shells on the front and back side of the tower. This achieves greater material savings while the number of structural joints remains the same. The resulting rectangular tower cross-section, such as shown in Fig. 1, is appropriate for a load-direction-derived design, such as mentioned in Section 1.2.

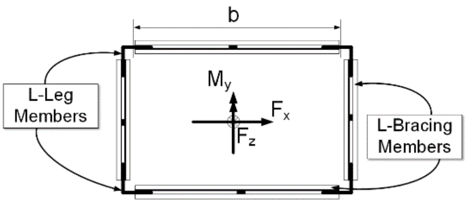

Fig. 1 Simplified rectangular cross-section of a rotatable lattice tower

The tower cross section can be sized according to its different bending stiffness requirements along the two main load directions by adjusting the main leg distances. For conventional, nonrotatable lattice tower concepts, the leg distance is constrained by blade-tower clearance requirements for any yaw orientation of the RNA. In contrast, the leg distance of a rotatable lattice structure does not have such constraints. Larger leg distances decrease their internal normal forces (N_{Leg}). This can easily be shown by observing Fig. 1 and Eq. 1, where M_{y} is the acting bending moment around the y-axis and b is the leg distance according to Petersen [9]

$$N_{\mathrm{Leg}} = \pm \frac{M_{\mathrm{y}}}{2\,b} - \frac{F_{\mathrm{z}}}{4}. \qquad (1)$$

In Eq1 $F_{\mathrm{z}}/4$ is subtracted to account for the self-weight induced axial force. Buckling lengths of the bracing members, however, are increased, but this negative aspect is partially compensated by employing a shallower brace angle α_{b}, as shown in Fig. 2. A lower α_{b} is realizable by an increasing number of X-braces along the tower. Normal bracing forces caused by shear force F_{x} are calculated by Eq. 2

$$N_{\mathrm{Brace}} = \frac{F_{\mathrm{x}}}{2\,\cos(\alpha_{\mathrm{b}} \pm \alpha_{\mathrm{y}})}, \qquad (2)$$

where α_{y} is the tower inclination angle. Note that its sign depends on the considered member in an X-bracing. In the case of torsional moments, additional normal stresses within the legs due to constrained warping would occur, which effectively increase the torsional stiffness of the structure. To capture this effect and the member loads within an aero-servo-elastic simulation, FEM should be used. Note that different tower-bending stiffnesses around the main x- and y-axes lead to two different bending modes, with a lower natural frequency for the bending around the x-axis. Considering the different member lengths and dimensions, a stiff-stiff design philosophy could be followed, where the lowest natural frequency is higher than the three-per-revolution excitation frequency within the operational range.

3.2 Advanced Economic Significance

Besides the increased material and cost efficiency of the legs, a slight inclination of the tower, such as shown in Fig. 2, leads to even greater blade-tower clearance, which may enable more economical blades. Summarizing the aspects of this and the previous section, the presented conceptual improvements indicate that a rotatable lattice tower meets the requirements of an innovative, environmentally friendly, and economic alternative to existing nonrotatable and rotatable approaches.

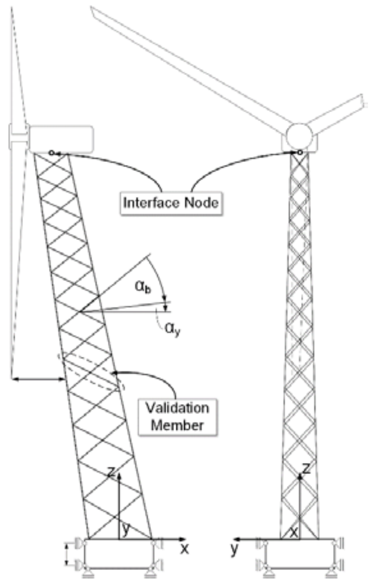

Fig. 2 Rotatable lattice tower concept

4. Preparations for Future Certifications

4.1 Modification of SubDyn

A way to analyze and verify the proposed design through aero-servo-elastic simulations is given by modification of the state-of-the-art, open-source, lattice-tower FEM module SubDyn [10]. Its coupling to the engineering tool FAST achieves aero-hydro-servo-elastic load simulations for resolved lattice support structures in land-based and offshore situations. SubDyn is capable of representing the structure through a linear-frame, finite-element beam model and a dynamic system reduction via the Craig-Bampton method. Furthermore, the application of a static-improvement method reduces the number of necessary modes to obtain accurate solutions [10]. Up until now, circular members were the only accepted member cross sections in the module. SubDyn was modified to account for arbitrary member cross sections, such as asymmetrical L-profiles, which are common for land-based lattice towers. Necessary changes took place in the structural beam element formulation. In the case of an isotropic straight beam with an arbitrary cross section, the centroid may not lie at the same position as the shear center and the principal bending and principal shear axes may not be parallel. These conditions introduce additional terms in the cross-sectional stiffness and mass matrices $\underline{\underline{K_c}}^{6\times6}$ and $\underline{\underline{M_c}}^{6\times6}$, which must be integrated along the element. Shape functions are used to describe the deflections and rotations of the beam at each position. Many approaches for the derivation of shape functions do exist, such as those described in [11], [12] and [13]. Taeseong, K. et al. [13] assume that the shape functions are polynomials of arbitrarily high order, where the corresponding coefficients are extractable by minimizing the elastic energy U of the entire beam under prescribed constraints at the beam ends. The elastic beam energy is calculated by integration over the whole beam element length L with

$$U = \frac{1}{2}\int_0^L \left(\underline{\varepsilon}^T \, \underline{\underline{K_c}} \, \underline{\varepsilon}\right) dz, \tag{3}$$

where $\underline{\varepsilon} = \{\gamma_{\mathrm{zx}}, \gamma_{\mathrm{zy}}, \varepsilon_{\mathrm{z}}, \kappa_{\mathrm{x}}, \kappa_{\mathrm{y}}, \kappa_{\mathrm{z}}\}^T$ is the strain vector of the Timoshenko beam with shear strains γ_{zx} and γ_{zy}, axial strain ε_{z}, and curvatures $\kappa_{\mathrm{x}}, \kappa_{\mathrm{y}}$, and κ_{z}. After introducing the shape function matrices into Eq. 3, considering the boundary conditions, and carrying out mathematical transformations, Taeseong, K. et al. [13] derived the following equations for beam element stiffness and mass matrices

$$\underline{\underline{K}}_{\mathrm{el}} = \underline{\underline{N}}_{\alpha}^T \left[\int_0^L \left(\underline{\underline{B}}^T \, \underline{\underline{K_c}} \, \underline{\underline{B}}\right) dz\right] \underline{\underline{N}}_{\alpha} \tag{4}$$

$$\underline{\underline{M}}_{\mathrm{el}} = \underline{\underline{N}}_{\alpha}^T \left[\int_0^L \left(\underline{\underline{N}}(z)^T \, \underline{\underline{M_c}} \, \underline{\underline{N}}(z)\right) dz\right] \underline{\underline{N}}_{\alpha}, \tag{5}$$

where $\underline{\underline{N}}_{\alpha}^{6p\times12}$ is the transformation matrix for the generalized degrees of freedom vector with $p-1$ as the highest power of the assumed polynomials. $\underline{\underline{N}}(z)^{6\times6p}$ is the polynomial matrix and $\underline{\underline{B}}^{6\times6p}$ is the strain-displacement matrix. This approach can be used for anisotropic curved beams with arbitrary cross sections, such as wind turbine blades. Therefore, it indicates more generality than necessary for the purpose of isotropic straight beams with arbitrary cross sections, which are common for lattice structures. On the other hand, either engineering constants or full six-by-six cross-sectional stiffness and mass matrices $\underline{\underline{K_c}}^{6\times6}$ and $\underline{\underline{M_c}}^{6\times6}$ can be defined for each member in the structure and may be useful for future research projects considering composite beams. Another important aspect is the cross-sectional orientation with respect to the beam axis in the case of arbitrary cross sections. Therefore, the direction cosine matrix $\underline{\underline{D}}_{\Phi\theta\psi}^{[\mathcal{F}_{SS}]}$ is used to transform the local element orthonormal basis $\mathcal{F}_{\mathrm{e}} = \left(\hat{\underline{\imath}}_{\mathrm{e}}, \hat{\underline{\jmath}}_{\mathrm{e}}, \hat{\underline{k}}_{\mathrm{e}}\right)$ into the global orthonormal basis $\mathcal{F}_{\mathrm{SS}} = \left(\hat{\underline{I}}, \hat{\underline{J}}, \hat{\underline{K}}\right)$ by Eq. 6

$$\begin{Bmatrix} \hat{\underline{\imath}}_{\mathrm{e}}^{[\mathcal{F}_{\mathrm{SS}}]} \\ \hat{\underline{\jmath}}_{\mathrm{e}}^{[\mathcal{F}_{\mathrm{SS}}]} \\ \hat{\underline{k}}_{\mathrm{e}}^{[\mathcal{F}_{\mathrm{SS}}]} \end{Bmatrix}^T = \underline{\underline{D}}_{\Phi\theta\psi}^{[\mathcal{F}_{\mathrm{SS}}]} \begin{Bmatrix} \hat{\underline{I}}^{[\mathcal{F}_{\mathrm{SS}}]} \\ \hat{\underline{J}}^{[\mathcal{F}_{\mathrm{SS}}]} \\ \hat{\underline{K}}^{[\mathcal{F}_{\mathrm{SS}}]} \end{Bmatrix}^T, \tag{6}$$

where the unit vectors $\hat{\underline{I}}, \hat{\underline{J}}, \hat{\underline{K}}$ and $\hat{\underline{\imath}}_{\mathrm{e}}, \hat{\underline{\jmath}}_{\mathrm{e}}, \hat{\underline{k}}_{\mathrm{e}}$ represent the axes of the Cartesian coordinate systems and are given with respect to $\mathcal{F}_{\mathrm{SS}}$. The corresponding direction cosine matrix is assembled from three planar rotations around the Euler angles Φ, θ, and ψ, according to

$$\underline{\underline{D}}_{\Phi\theta\psi}^{[\mathcal{F}_{\mathrm{SS}}]} = \underline{\underline{D}}_{\Phi}^{[\mathcal{F}_{\mathrm{SS}}]} \, \underline{\underline{D}}_{\theta}^{[\mathcal{F}_1]} \, \underline{\underline{D}}_{\psi}^{[\mathcal{F}_2]}$$
$$= \begin{bmatrix} C_\Phi C_\psi - S_\Phi C_\theta S_\psi & -C_\Phi S_\psi - S_\Phi C_\theta C_\psi & S_\Phi S_\theta \\ S_\Phi C_\psi + C_\Phi C_\theta S_\psi & -S_\Phi S_\psi + C_\Phi C_\theta C_\psi & -C_\Phi S_\theta \\ S_\theta S_\psi & S_\theta C_\psi & C_\theta \end{bmatrix}, \tag{7}$$

where $\underline{\underline{D}}_{\Phi}^{[\mathcal{F}_{\mathrm{SS}}]}$, $\underline{\underline{D}}_{\theta}^{[\mathcal{F}_1]}$, and $\underline{\underline{D}}_{\psi}^{[\mathcal{F}_2]}$ represent the direction cosine matrices for each of these rotations with respect to their local orthonormal bases [14]. The abbreviations S and C are representative for the geometric sine and cosine functions, and its indexes show its corresponding Euler angle arguments. Angle ψ in Eq. 7 is the cross-sectional orientation angle around the beam axis and is directly definable by the user. Another way to define the orientation is given through a representative unit vector for the local member cross-sectional x-axis, introduced through a user-prescribed point, which will be projected to a plane orthogonal to the member axis.

4.2 Validation of Changes in SubDyn

To validate the changes applied to SubDyn, a parallel-modelling approach with the finite-element software Abaqus (version 2016) was conducted. The lattice tower, shown in Fig. 2, was modeled in both software packages. A prescribed static-load case and a frequency analysis were performed, and certain member loads and the natural frequencies of the entire structure were compared within both models. L-beam dimensions were calculated via a Python script, which coupled an Artificial Bee Colony [15] optimization algorithm to Abaqus. Nevertheless, exact dimensions of the members are not required to validate the changes in SubDyn. In the validation load case, the lattice tower was fixed at the bottom and displacements and rotations at the tower-to-nacelle interface node, shown in Fig. 2, were applied according to Table 1.

u_{x}	u_{y}	u_{z}	ur_{x}	ur_{y}	ur_{z}
$0.1\,m$	$0.1\,m$	$0.1\,m$	$0.1\,rad$	$0.1\,rad$	$0.1\,rad$

Tab. 1 Prescribed displacements and rotations at the tower top for validation of member loads

Fig. 3 shows the results of this load case in the form of member load components for the two members of the fifth bracing level, marked in Fig. 2. Good agreement between both models for each load component can be seen. In Abaqus, 24 elements were used for each member. In contrast, the rigorous beam-element approach applied in SubDyn leads to good performance with only two elements per member. Even one element would produce the same results in SubDyn, but two elements have been selected to compare not only loads at the joint nodes of each member, but also at their midpoints. Other structure members show similar good agreement.

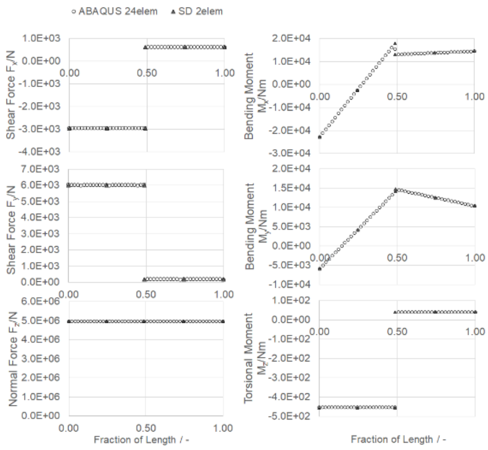

Fig. 3 Local loads of two members of the fifth bracing level along their fractional length in Abaqus and SubDyn as a result of prescribed displacements and rotations, given in Tab. 1, at the interface node

The frequency analysis results, shown in Fig.4, are produced by a 32-element discretization in Abaqus and different discretization levels in SubDyn. All of the first 10 natural frequencies are in good agreement and their maximum differences between both models are $\leq 2.193\,\%$ for one element, $\leq 0.317\,\%$ for two elements, and $\leq 0.129\,\%$ for three elements. Higher modes show insignificant higher discrepancies. These results indicate that not only the beam stiffness, but also the mass matrix implementations are correct.

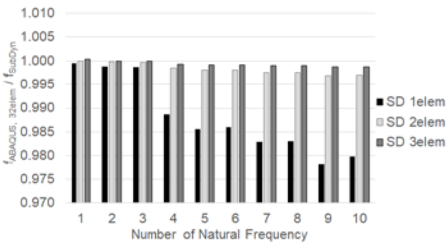

Fig. 4 Natural frequency ratios between Abaqus and SubDyn with different discretization levels

These validated changes in SubDyn make future certifications of rotatable lattice tower concepts viable and are also beneficial for other nonrotatable lattice structures.

5. Acknowledgements

This work was supported by the U.S. Department of Energy under Contract No. DE-AC36-08GO28308 with the National Renewable Energy Laboratory. Funding for the work was provided by the DOE Office of Energy Efficiency and Renewable Energy, Wind Energy Technologies Office.

The U.S. Government retains and the publisher, by accepting the article for publication, acknowledges that the U.S. Government retains a nonexclusive, paid-up, irrevocable, worldwide license to publish or reproduce the published form of this work, or allow others to do so, for U.S. Government purposes.
Furthermore, the present work was supported by the Energie und Klimaschutzgesellschaft Schleswig-Holstein.

6. References

[1] Gasch, R.: Wind Power Plants: Fundamentals, Design, Construction and Operation. 2. ed., Springer, Berlin, 2012.
[2] Penman, J.; Gytarsky, M.; Hiraishi, T.; Irving, W. and Krug T.: 2006 IPCC Guidelines for National Greenhouse Gas Inventories. World Meteorological Organization, United Nations Environment Programme, 2006.
[3] Rüster, D.: Mühlentechnik Windmühle in Abbenrode Zustand um 1910, Baukonstruktion. http://www.museumsmuehle-abbenrode.de/index.php?M%FChlentechnik, last view: 15. June 2017.
[4] Kleinhenz, F.: Denkschrift 6 - Das Großwindkraftwerk MAN-Kleinhenz (Erweiterter Abdruck aus ‚Der Bauingenieur' 1942, Heft 23/24, Kleinhenz: ‚Projekt eines Großwindkraftwerkes'). Manuscript. Berlin, 21. March 1943.
[5] Himmelmann, R.: Airfoil Design for Wakeless Wind Turbine Tower Structures. US20130156596A1, filed 19. December 2011, and issued 20. June 2013.
[6] Beye, T.; Rudolf, R. and Faber, T.: Konzeptstudie für Windenergieanlage mit Azimutlager am Turmfuß. Bauingenieur Band 88 (2013): 269–74.
[7] Steel Pro Maschinenbau: ASPARAGO Neue Türme für die Windenergie. Information brochure. Berlin, 2016.
[8] Himmelmann, R. and Tongue, S. E.: Hybrid Wind Turbine Tower with Integrated Yaw Bearing System. US20130171002A1, filed 29. Dezember 2011, and issued 4. July 2013.
[9] Petersen, C.: Stahlbau: Grundlagen der Berechnung und baulichen Ausbildung von Stahlbauten. 4. ed., Springer Vieweg, Wiesbaden, 2013.
[10] Damiani, R.; Jonkman, J. and Hayman, G.: SubDyn User's Guide and Theory Manual National Renewable Energy Laboratory, Golden, CO, March 2015.
[11] Przemieniecki, J. S.: Theory of matrix structural analysis. New York: Dover, 1985.
[12] Hodges, D. H.: Nonlinear Composite Beam Theory. Progress in Astronautics and Aeronautics 213. Reston, USA: American Institute of Aeronautics and Astronautics, 2006.
[13] Taeseong, K.; Hansen, A. M. and Branner K.: Development of an Anisotropic Beam Finite Element for Composite Wind Turbine Blades in Multibody System. Renewable Energy 59 (November 2013): 172–83. doi:10.1016/j.renene.2013.03.033.
[14] Bauchau, O. A.: Flexible Multibody Dynamics. Solid Mechanics and Its Applications 176. Springer, Atlanta, U.S., 2011.
[15] Karaboga, D. and Basturk, B.: A Powerful and Efficient Algorithm for Numerical Function Optimization: Artificial Bee Colony (ABC) Algorithm. Journal of Global Optimization 39, No. 3 (9. Oktober 2007): 459–71. doi:10.1007/s10898-007-9149-x.